nature immunology

Repression of the genome organizer SATB1 in regulatory T cells is required for suppressive function and inhibition of effector differentiation

Marc Beyer[1], Yasser Thabet[1], Roman-Ulrich Müller[2,3], Timothy Sadlon[4], Sabine Classen[1], Katharina Lahl[5], Samik Basu[6], Xuyu Zhou[7], Samantha L Bailey-Bucktrout[7], Wolfgang Krebs[1], Eva A Schönfeld[1], Jan Böttcher[8], Tatiana Golovina[6], Christian T Mayer[5], Andrea Hofmann[1], Daniel Sommer[1], Svenja Debey-Pascher[1], Elmar Endl[8], Andreas Limmer[8], Keli L Hippen[9], Bruce R Blazar[9], Robert Balderas[10], Thomas Quast[11], Andreas Waha[12], Günter Mayer[13], Michael Famulok[13], Percy A Knolle[8], Claudia Wickenhauser[14], Waldemar Kolanus[11], Bernhard Schermer[2,3], Jeffrey A Bluestone[7], Simon C Barry[4], Tim Sparwasser[5], James L Riley[6] & Joachim L Schultze[1]

Regulatory T cells (T_{reg} cells) are essential for self-tolerance and immune homeostasis. Lack of effector T cell (T_{eff} cell) function and gain of suppressive activity by T_{reg} cells are dependent on the transcriptional program induced by Foxp3. Here we report that repression of SATB1, a genome organizer that regulates chromatin structure and gene expression, was crucial for the phenotype and function of T_{reg} cells. Foxp3, acting as a transcriptional repressor, directly suppressed the *SATB1* locus and indirectly suppressed it through the induction of microRNAs that bound the *SATB1* 3′ untranslated region. Release of *SATB1* from the control of Foxp3 in T_{reg} cells caused loss of suppressive function, establishment of transcriptional T_{eff} cell programs and induction of T_{eff} cell cytokines. Our data support the proposal that inhibition of SATB1-mediated modulation of global chromatin remodeling is pivotal for maintaining T_{reg} cell functionality.

Regulatory T cells (T_{reg} cells) are characterized by their suppressive function and inability to produce effector cytokines after activation[1]. Expression of the X-linked forkhead transcription factor Foxp3 has been linked to the establishment and maintenance of the identity and suppressor function of the T_{reg} cell lineage[2–7]. Moreover, Foxp3 is also associated with the control of effector T cell (T_{eff} cell) function in T_{reg} cells[4,5]. A growing body of evidence has indicated plasticity among committed $CD4^+$ T cell lineages, including T_{reg} cells[8–11], yet the mechanism of this plasticity and its importance in normal immune responses and disease states remain to be elucidated.

Many transgenic reporter mouse models have demonstrated that loss of Foxp3 can induce the conversion of T_{reg} cells into cells with a variety of T_{eff} cell programs[2–4,12]. Although T_{reg} cells are reprogrammed by loss of the lineage-associated transcription factor Foxp3, there is no evidence that conventional T cells (T_{conv} cells) actively suppress the T_{reg} cell lineage program. In contrast, only stable expression of Foxp3 in T_{conv} cells seems able to induce a T_{reg} cell phenotype in these cells[7]. Together these findings suggest that T_{eff} cell programs are the default state in $CD4^+$ T cells and that transcriptional programs induced and maintained by Foxp3 over-rule T_{eff} cell function in T_{reg} cells[5]. Whether the inhibition of T_{eff} cell differentiation in T_{reg} cells is critical for the suppressive function of T_{reg} cells is unclear. Such a model would be supported by evidence showing the existence of Foxp3-induced mechanisms that continuously and actively control T_{eff} cell programs in these specialized T cells.

Consistent with the active suppression of T_{eff} cell programs in T_{reg} cells, ablation of the transcriptional repressor Eos[13] or the Foxo transcription factors[14,15] imparts partial T_{eff} cell characteristics to

[1]Life and Medical Sciences Institute, Laboratory for Genomics and Immunoregulation, University of Bonn, Bonn, Germany. [2]Renal Division, Department of Medicine and Centre for Molecular Medicine, University of Cologne, Cologne, Germany. [3]Cologne Excellence Cluster on Cellular Stress Responses in Aging-Associated Diseases, University of Cologne, Cologne, Germany. [4]Discipline of Paediatrics, Women's and Children's Health Research Institute, University of Adelaide, North Adelaide, Australia. [5]Institute of Infection Immunology, TWINCORE, Centre for Experimental and Clinical Infection Research, a joint venture between the Medical School Hannover and the Helmholtz Centre for Infection Research, Hannover, Germany. [6]Department of Microbiology, Translational Research Program, Abramson Family Cancer Research Institute, University of Pennsylvania, Philadelphia, Philadelphia, USA. [7]Diabetes Center and the Department of Medicine, University of California, San Francisco, California, USA. [8]Institutes of Molecular Medicine and Experimental Immunology, University Hospital Bonn, Bonn, Germany. [9]Cancer Center and Department of Pediatrics, Division of Blood and Marrow Transplantation, University of Minnesota, Minneapolis, Minnesota, USA. [10]BD Biosciences–Pharmingen, San Diego, California, USA. [11]Life and Medical Sciences Institute, Laboratory for Molecular Immunology, University of Bonn, Bonn, Germany. [12]Department of Neuropathology, University Hospital Bonn, Bonn, Germany. [13]Life and Medical Sciences Institute, Laboratory of Chemical Biology, University of Bonn, Bonn, Germany. [14]Department for Diagnostic, Institute for Pathology, University Hospital Leipzig, Leipzig, Germany. Correspondence should be addressed to J.L.S. (j.schultze@uni-bonn.de).

Received 24 May; accepted 7 July; published online 14 August 2011; doi:10.1038/ni.2084

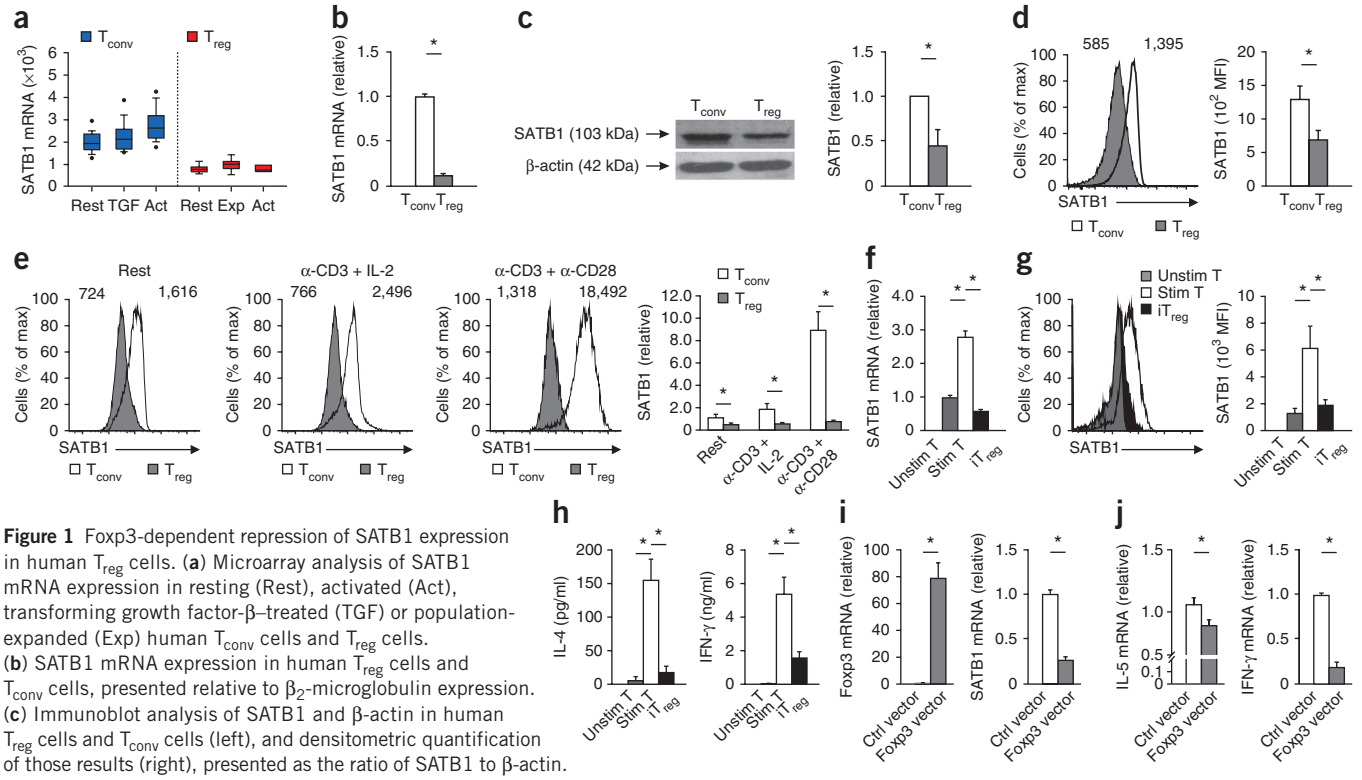

Figure 1 Foxp3-dependent repression of SATB1 expression in human T_{reg} cells. (**a**) Microarray analysis of SATB1 mRNA expression in resting (Rest), activated (Act), transforming growth factor-β–treated (TGF) or population-expanded (Exp) human T_{conv} cells and T_{reg} cells. (**b**) SATB1 mRNA expression in human T_{reg} cells and T_{conv} cells, presented relative to β_2-microglobulin expression. (**c**) Immunoblot analysis of SATB1 and β-actin in human T_{reg} cells and T_{conv} cells (left), and densitometric quantification of those results (right), presented as the ratio of SATB1 to β-actin. (**d**) Flow cytometry analysis of SATB1 expression in human T_{reg} cells and T_{conv} cells (left), and quantification of those results (right), presented as mean fluorescence intensity (MFI). (**e**) Flow cytometry analysis of SATB1 expression in human T_{reg} cells and T_{conv} cells left unstimulated (resting cells (Rest)) or stimulated for 2 d with anti-CD3 and IL-2 (α-CD3 + IL-2) or anti-CD3 and anti-CD28 (α-CD3 + α-CD28; left), and quantification of those results (right), presented as normalized results relative to those in resting T_{conv} cells. (**f**) SATB1 mRNA expression in human iT_{reg} cells and T cells stimulated with anti-CD3 and anti-CD28 (Stim T) and unstimulated T cells (Unstim T) on day 5, presented as in **b**. (**g**) Flow cytometry analysis of SATB1 expression in cells as in **f** (left), and quantification of those results (right), presented as in **d**. (**h**) Cytometric bead assay of IL-4 and IFN-γ in the supernatants of cells as in **f**. (**i**) Expression of Foxp3 and SATB1 mRNA in T_{conv} cells transduced with lentivirus containing a vector encoding Foxp3 (Foxp3 vector) or control vector (Ctrl vector), then allowed to 'rest' for 3 d; results presented as in **b**. (**j**) Expression of IL-5 and IFN-γ mRNA, assessed and presented as in **i**. Numbers in plots (**d**,**e**) indicate mean fluorescence intensity. *$P < 0.05$ (Student's *t*-test). Data are representative of at least eight experiments per group (**a**), or five (**b**,**e**,**i**,**j**), six (**c**,**f**), three (**g**) or eleven (**d**) experiments (mean and s.d.) or three independent experiments (**h**; mean and s.d. of triplicate wells), each with cells derived from a different donor.

T_{reg} cells. Other transcription factors, including IRF4 (ref. 16) and STAT3 (ref. 17), have been linked to the modulation of effector cell differentiation by T_{reg} cells[18]. There is evidence that epigenetic control, as well as microRNA (miRNA), is important for Foxp3-mediated suppressive functions[16,19–23], which raises the possibility that epigenetic and post-transcriptional regulation may also be involved in the repression of T_{eff} cell functions in T_{reg} cells. These findings support the proposal of the existence of active regulatory mechanisms that enable committed T_{reg} cells to suppress their differentiation into T_{eff} cells[24].

In this report, we specifically searched for genes repressed by Foxp3 in T_{reg} cells that might be central to maintaining regulatory function and the suppression of T_{eff} cell function in T_{reg} cells. We identified the gene encoding the genome organizer SATB1 among the genes most repressed in human and mouse T_{reg} cells. SATB1 is a chromatin organizer and transcription factor essential for the control of a large number of genes that participate in T cell development and activation[25]. SATB1 regulates gene expression by directly recruiting chromatin-modifying factors to the loci of its target genes, which are tethered to the SATB1 regulatory network via specialized genomic sequences called 'base-unpairing regions'[26–28]. In mouse T helper type 2 (T_H2) clones, SATB1 has been shown to function as a global transcriptional regulator that specifically anchors the looped topology of the locus encoding T_H2 cytokines, a prerequisite for the induction of T_H2 cytokines[29]. As SATB1-deficient thymocytes do not develop beyond the double-positive ($CD4^+CD8^+$) stage[25,26], the role of SATB1 in peripheral T cells, particularly in T_{reg} cells, has remained elusive. Here we found that repression of SATB1 in T_{reg} cells was mediated directly by transcriptional control of Foxp3 at the *SATB1* locus, through maintenance of a repressive chromatin state at this locus, and indirectly by Foxp3-dependent miRNAs. Release of *SATB1* from Foxp3 control was sufficient to reprogram natural $Foxp3^+$ T_{reg} cells into T_{eff} cells that lost suppressive function and gained T_{eff} cell function. Our findings show that control of *SATB1* by Foxp3 is an essential and critical mechanism that maintains T_{reg} cell functionality.

RESULTS

Low expression of SATB1 in human T_{reg} cells

To identify regulatory circuits actively suppressed by Foxp3 as a prerequisite for T_{reg} cell function and inhibition of T_{eff} cell programs, we did whole-transcriptome analysis of human resting or activated T_{conv} cells and natural T_{reg} cells (**Supplementary Fig. 1** and **Supplementary Table 1**). We identified SATB1 as one of 22 genes with significantly lower expression in T_{reg} cells than in T_{conv} cells (**Fig. 1a**). Reassessment of transcriptome data from published reports[30–32] confirmed our observation that *SATB1* was a potential target of Foxp3-mediated repression.

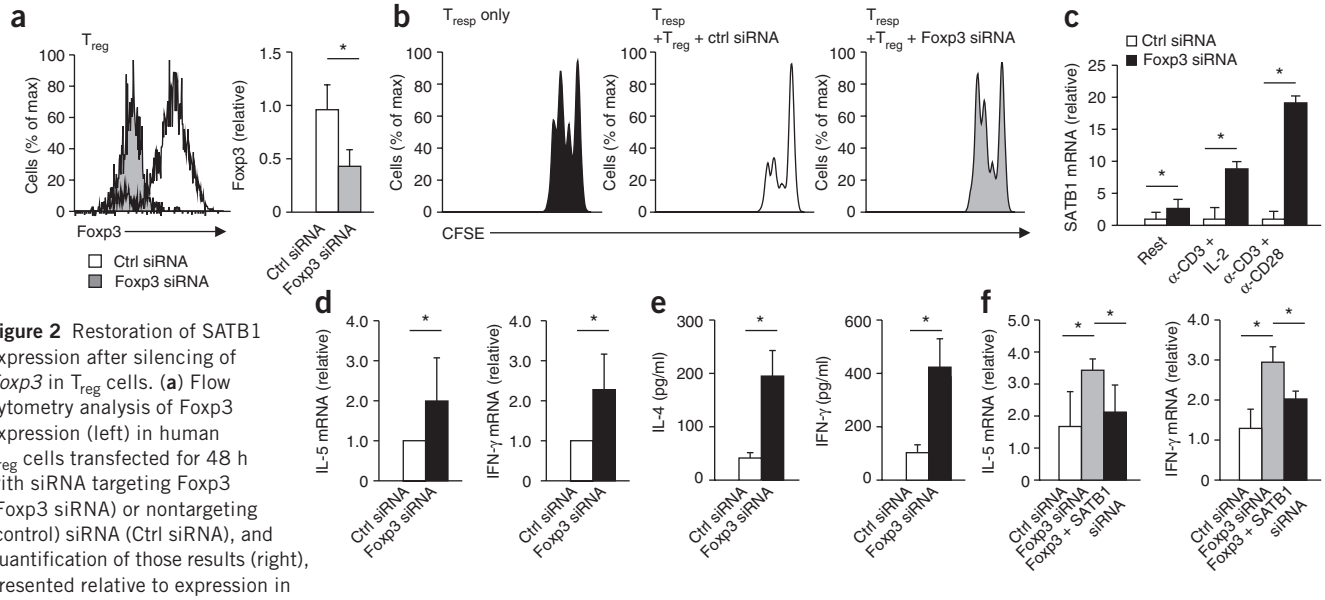

Figure 2 Restoration of SATB1 expression after silencing of *Foxp3* in T_{reg} cells. (**a**) Flow cytometry analysis of Foxp3 expression (left) in human T_{reg} cells transfected for 48 h with siRNA targeting Foxp3 (Foxp3 siRNA) or nontargeting (control) siRNA (Ctrl siRNA), and quantification of those results (right), presented relative to expression in control siRNA–transfected T_{reg} cells. (**b**) Suppression of allogeneic $CD4^+$ T cells labeled with the cytosolic dye CFSE (responding T cells (T_{resp})) by human T_{reg} cells transfected with siRNA as in **a**, presented as CFSE dilution in responding T cells cultured at a ratio of 1:1 with T_{reg} cells plus beads coated with anti-CD3 and anti-CD28, or without T_{reg} cells (T_{resp} only). (**c**) Expression of SATB1 mRNA in human T_{reg} cells transfected with siRNA as in **a**, then cultivated for 48 h without stimulation (Rest) or in the presence of anti-CD3 and IL-2 or beads coated with anti-CD3 and anti-CD28; results are presented relative to β_2-microglobulin expression. (**d**) Expression of IL-5 and IFN-γ mRNA in T_{reg} cells transfected with siRNA as in **a**, then stimulated for 48 h with anti-CD3 and IL-2; results presented as in **c**. (**e**) Cytometric bead assay of IL-4 and IFN-γ in supernatants of siRNA-treated T_{reg} cells stimulated as in **d**. (**f**) Expression of IL-5 and IFN-γ mRNA in T_{reg} cells transfected with nontargeting siRNA or siRNA targeting Foxp3 alone (Foxp3 siRNA) or both Foxp3 and SATB1 (Foxp3 + SATB1 siRNA), followed by stimulation for 48 h with beads coated with anti-CD3 and anti-CD28; results presented as in **c**. $^*P < 0.05$ (Student's *t*-test (**a**,**c**–**e**) or one-way analysis of variance with Fisher's least-significant-difference test (**f**)). Data are representative of six (**a**,**c**) or four (**d**,**f**) experiments (mean and s.d.) or three independent experiments (**b**,**e**; mean and s.d. of triplicate wells in **e**), each with cells derived from a different donor.

We confirmed the transcriptome data in an independent set of samples by quantitative RT-PCR (**Fig. 1b**), immunoblot analysis (**Fig. 1c**) and single-cell analysis by flow cytometry (**Fig. 1d**); this demonstrated lower SATB1 expression in human T_{reg} cells. As higher SATB1 expression has been linked to the activation of T cell populations[29,33], we assessed the dynamics of the expression of SATB1 protein in T_{conv} cells and T_{reg} cells during activation via stimulation of the T cell antigen receptor (TCR) in the presence of costimulation or interleukin 2 (IL-2; **Fig. 1e**), as well as mitogens (data not shown). Analysis of SATB1 expression demonstrated stimulation-dependent upregulation of SATB1 in T_{conv} cells, whereas resting T_{reg} cells had significantly lower SATB1 expression than T_{conv} cells had, and this expression was upregulated only modestly after T cell activation. Next we assessed SATB1 in induced T_{reg} cells (iT_{reg} cells)[34]. These cells expressed Foxp3 mRNA and protein and had T cell suppressive function (data not shown). Similar to natural T_{reg} cells, iT_{reg} cells did not show induction of SATB1, whereas cells stimulated via TCR and CD28 showed significantly enhanced expression (**Fig. 1f**,**g**). Moreover, the production of T_H1 and T_H2 cytokines was significantly abrogated in the absence of SATB1 (**Fig. 1h**). To determine whether Foxp3 induction in iT_{reg} cells was necessary to suppress *SATB1*, we did gain-of-function experiments using T_{conv} cells with ectopic overexpression of Foxp3. High expression of Foxp3 resulted in lower expression of SATB1 (**Fig. 1i**), accompanied by concomitantly lower cytokine expression (**Fig. 1j**) and the induction of a T_{reg} cell gene signature (**Supplementary Fig. 2**). Lower Foxp3 expression did not result in substantial repression of *SATB1* or induction of a T_{reg} cell gene signature (data not shown). Thus, lower SATB1 expression is a hallmark of both iT_{reg} cells and T_{reg} cells in humans, and repression of SATB1 depends on sufficiently high expression of Foxp3.

Loss of Foxp3 in T_{reg} cells results in high SATB1 expression

To further assess the role of Foxp3 in SATB1 repression in human T_{reg} cells, we did loss-of-function experiments. Silencing Foxp3 via small interfering RNA (siRNA) resulted in loss of Foxp3 expression as well as the expression of genes associated with T_{reg} cells (**Supplementary Fig. 3**) and, consequently, loss of suppressive function in T_{reg} cells (**Fig. 2a**,**b**). Slightly but significantly higher SATB1 expression was evident in unstimulated human T_{reg} cells depleted of Foxp3 (**Fig. 2c**); however, this was significantly enhanced in T_{reg} cells stimulated via the TCR together with costimulation or IL-2. This higher SATB1 expression was associated with the production of T_H1 cytokines (interferon-γ (IFN-γ)) and T_H2 cytokines (IL-4 and IL-5; **Fig. 2d**,**e**). As this effect could have been a direct effect of Foxp3 on the cytokine-encoding genes themselves, we developed a strategy to knock down SATB1 and Foxp3 simultaneously in human T_{reg} cells. Additional knockdown of SATB1 in human T_{reg} with a silenced *Foxp3* gene (**Supplementary Fig. 4**) resulted in significantly less induction of helper T cell cytokines (**Fig. 2f**), which demonstrated that the expression of T_{eff} cell cytokines in Foxp3-deficient T_{reg} cells was governed by SATB1. We obtained similar results when we transduced expanded human T_{reg} cell populations with lentivirus encoding miRNA targeting Foxp3 and SATB1 for RNA-mediated interference (**Supplementary Fig. 5**). Together these findings establish that Foxp3 negatively regulates SATB1 expression and that lower SATB1 expression is needed to prevent expression of T_{eff} cell cytokines in human T_{reg} cells, which therefore assigns a key function of Foxp3-SATB1 interaction to the T_{reg} cell phenotype.

No suppression of Foxp3 by SATB1 in T_{conv} cells

To exclude the possibility that SATB1 reciprocally repressed *Foxp3* in T_{conv} cells, we did siRNA-mediated knockdown of SATB1 in human

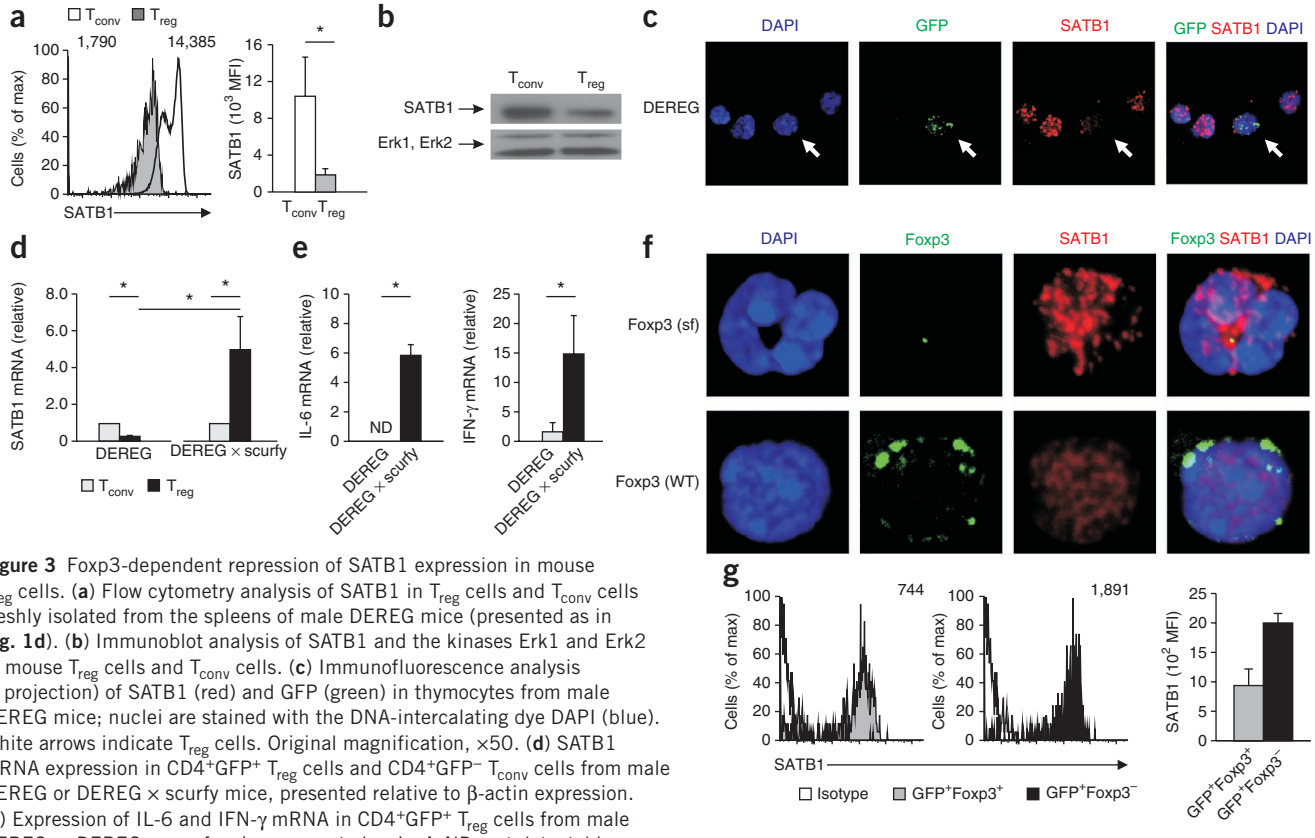

Figure 3 Foxp3-dependent repression of SATB1 expression in mouse T_{reg} cells. (**a**) Flow cytometry analysis of SATB1 in T_{reg} cells and T_{conv} cells freshly isolated from the spleens of male DEREG mice (presented as in **Fig. 1d**). (**b**) Immunoblot analysis of SATB1 and the kinases Erk1 and Erk2 in mouse T_{reg} cells and T_{conv} cells. (**c**) Immunofluorescence analysis (*z* projection) of SATB1 (red) and GFP (green) in thymocytes from male DEREG mice; nuclei are stained with the DNA-intercalating dye DAPI (blue). White arrows indicate T_{reg} cells. Original magnification, ×50. (**d**) SATB1 mRNA expression in $CD4^+GFP^+$ T_{reg} cells and $CD4^+GFP^-$ T_{conv} cells from male DEREG or DEREG × scurfy mice, presented relative to β-actin expression. (**e**) Expression of IL-6 and IFN-γ mRNA in $CD4^+GFP^+$ T_{reg} cells from male DEREG or DEREG × scurfy mice, presented as in **d**. ND, not detectable. (**f**) Confocal microscopy of SATB1 (red) and Foxp3 (green) in thymic $CD4^+GFP^+Foxp3^-$ T_{reg} cells (Foxp3 (sf)) or $CD4^+GFP^+Foxp3^+$ T_{reg} cells (Foxp3 (WT)) from female DEREG mice heterozygous for the scurfy mutation ($n = 25$ cells), counterstained with DAPI (blue). Original magnification, ×240. (**g**) Flow cytometry analysis of SATB1 expression in thymic T_{reg} cells as in **f** (presented as in **Fig. 1d**). Isotype, isotype-matched control antibody. $^*P < 0.05$ (Student's *t*-test). Data are representative of three independent experiments (**a**,**f**; mean and s.d.) or two independent experiments (**b**–**e**,**g**; mean and s.d. in **g** and mean and s.d. of triplicate wells in **d**,**e**).

naive T_{conv} cells to assess whether SATB1 downregulation in T_{conv} cells allowed higher Foxp3 expression and the conversion of T_{conv} cells into T_{reg} cells (**Supplementary Fig. 6a**). We did not observe higher Foxp3 expression in resting or stimulated naive T_{conv} cells after silencing of *SATB1*, even in iT_{reg} cell–inducing conditions (**Supplementary Fig. 6b**). These results suggest that SATB1 is not necessary for low expression of Foxp3 in resting T_{conv} cells and that Foxp3 induction in naive T_{conv} cells after stimulation occurs independently of SATB1. In line with that finding, we did not observe induction of several T_{reg} cell–associated genes after knockdown of SATB1 (**Supplementary Fig. 6c**).

SATB1 expression in mouse T_{reg} cells

To address whether regulation of the gene encoding SATB1 is conserved in human and mouse T_{reg} cells, we analyzed SATB1 expression by quantitative PCR, immunoblot analysis, flow cytometry and confocal microscopy in T cells derived from two different Foxp3 reporter mice (DEREG mice (which express green fluorescent protein (GFP) under control of the *Foxp3* promoter)[35] and Foxp3-GFP-Cre mice[21]). Similar to their expression in human T_{reg} cells, expression of SATB1 mRNA and protein was lower in mouse T_{reg} cells than in T_{conv} cells isolated from thymus, spleen or lymph nodes (**Fig. 3a**–**c** and data not shown). SATB1 expression was much higher in $CD4^+$ single-positive thymocytes than in peripheral $CD4^+$ T_{conv} cells from the spleen or lymph nodes (data not shown), which further supported the idea of an essential role for SATB1 during early thymocyte development, as established in mice completely deficient in SATB1 ($Satb1^{-/-}$ mice)[25]. Despite that, thymic $Foxp3^+$ T_{reg} cells still had substantial downregulation of SATB1 relative to its expression in $Foxp3^-$ cells.

To establish *Satb1* as a target of Foxp3, we analyzed T_{reg} cells from male DEREG mice with a spontaneously mutated *Foxp3* allele (DEREG × scurfy mice). Flow cytometry–sorted T_{reg} cells from these mice had significantly higher SATB1 expression in T_{reg} cells than Foxp3-sufficient T_{reg} cells had (**Fig. 3d**). In line with that finding, we found more T_H1 and T_H2 cytokines *in vivo* in T_{reg} cells from DEREG × scurfy mice (**Fig. 3e**). We further confirmed the difference in SATB1 mRNA expression in Foxp3-sufficient versus FOXP3-deficient T_{reg} cells by reassessing two transcriptome data sets derived from mice with a mutated *Foxp3* gene in T_{reg} cells[5,36] (Gene Expression Omnibus accession codes GSE6681 and GSE11775; data not shown).

Female heterozygous DEREG × scurfy mice have both GFP^+ Foxp3-sufficient and GFP^+ Foxp3-deficient T_{reg} cells. Side-by-side comparison of these cells by immunofluorescence demonstrated a cell-intrinsic function for Foxp3 in the repression of SATB1 (**Fig. 3f**). Similar to published reports[26], we observed nuclear localization of SATB1 in $Foxp3^-$ thymocytes in which SATB1 formed a cage-like structure (**Fig. 3c**). The finding of more SATB1 in Foxp3-deficient T_{reg} cells with unchanged localization and distribution further supported the proposal that SATB1 expression was regulated by Foxp3 (**Fig. 3f**). We further quantified the upregulation of SATB1 in GFP^+ $Foxp3^-$ T_{reg} cells by intracellular flow cytometry (**Fig. 3g**). Overall, these data established higher expression of SATB1 mRNA and protein as a consequence of Foxp3 deficiency in T_{reg} cells.

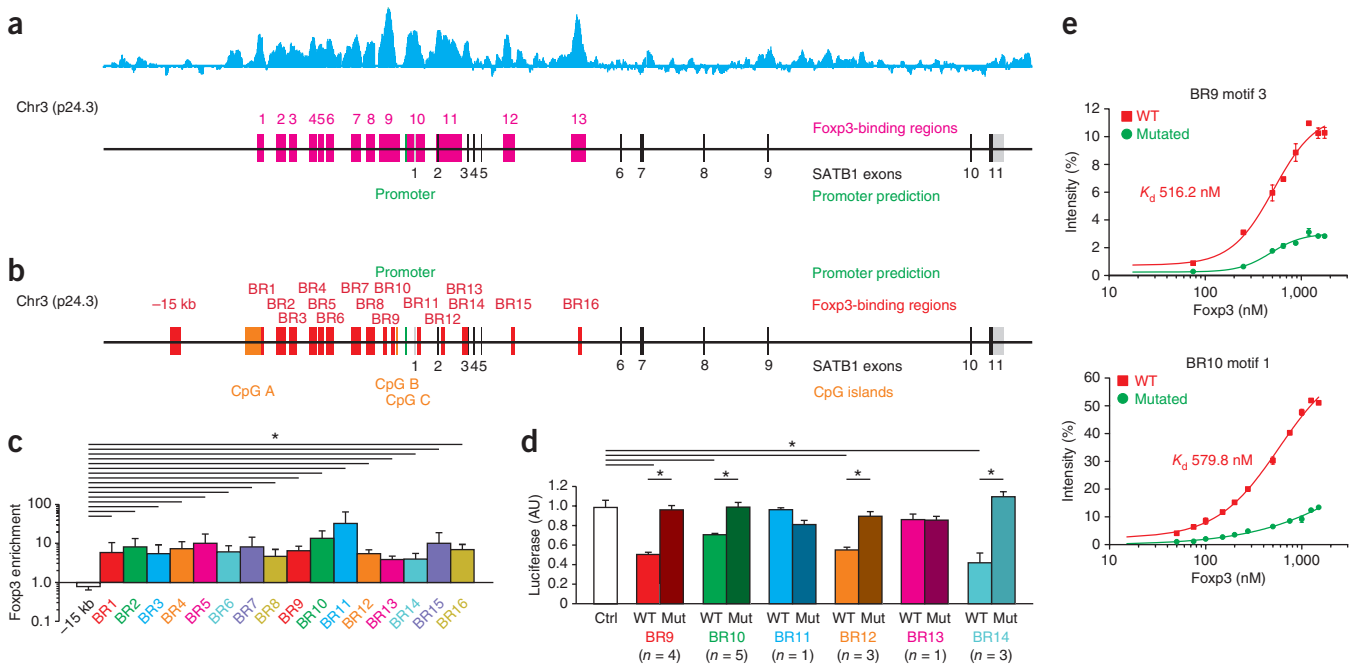

Figure 4 Direct suppression of *SATB1* transcription by Foxp3. (**a**) Foxp3 ChIP tiling array data from expanded populations of human cord blood–derived T_{reg} cells (blue; top), analyzed by model-based analysis of tiling array and overlaid onto the *SATB1* locus for identification of binding regions (1–13 (magenta); $P < 10^{-5}$; false-discovery rate < 0.5%). Chr3, chromosome 3. (**b**) Foxp3-binding regions (BR1–BR16) in the human genomic *SATB1* locus, identified by *in silico* prediction in the regions identified in **a**. (**c**) ChIP analysis of expanded populations of human cord blood–derived T_{reg} cells with a Foxp3-specific antibody and PCR primers specific for Foxp3-binding regions; results are presented relative to input, normalized to immunoglobulin G. −15 kb (far left), region 15 kb upstream of the transcription start site (negative control). $^*P < 0.05$, each binding region versus the negative control (horizontal lines at top; Student's *t*-test). (**d**) Luciferase assay of the binding of Foxp3 to binding regions in the *SATB1* locus in HEK293T cells transfected with luciferase constructs containing wild-type (WT) or mutated (Mut) binding regions BR9–BR14 of the *SATB1* locus (with mutation of the Foxp3-binding motifs) or control vector (Ctrl), together with a Foxp3 expression vector; results are presented in arbitrary units (AU) relative to those obtained with control vector. Numbers below graph indicate total Foxp3-binding motifs in each region. $^*P < 0.05$, experimental versus control (top) or wild-type versus mutated (directly above bars; Student's *t*-test). (**e**) Filter-retention analysis of the binding of Foxp3 to a wild-type or mutated Foxp3-binding motif in binding region 9 or 10 of the *SATB1* locus; numbers in plots indicate dissociation constant (K_d). Data are representative of two (**a**) or three (**c**,**e**) independent experiments with cells derived from different donors (mean and s.d. in **c** and mean and s.d. of triplicates in **e**) or one experiment representative of two (**d**; mean and s.d. of triplicate wells).

Binding of Foxp3 to the *SATB1* locus in human T_{reg} cells

The inverse correlation between Foxp3 expression and SATB1 expression in mouse and human T_{reg} cells suggested that Foxp3 might act directly as a transcriptional repressor of the *SATB1* locus. We did chromatin immunoprecipitation (ChIP) tiling arrays and promoter arrays of Foxp3 using chromatin isolated from human natural T_{reg} cells (**Fig. 4a** and **Supplementary Fig. 7a**) as well as bioinformatics *in silico* prediction to identify 16 regions for confirmation by quantitative PCR. The Foxp3-binding regions identified were located upstream of the transcriptional start site as well as in the genomic locus of *SATB1* (**Fig. 4b** and **Supplementary Table 2**). We demonstrated binding of Foxp3 to the promoter region or genomic locus of *SATB1* in T_{reg} cells by ChIP-coupled quantitative PCR (**Fig. 4c**) and electrophoretic mobility-shift assays (data not shown), which showed binding to the *SATB1* locus similar to that of known targets of Foxp3 (**Supplementary Fig. 7b–f**). To probe the functional consequences of the binding of Foxp3 to the *SATB1* locus, we did luciferase reporter assays for six of the Foxp3-binding regions. We cloned these Foxp3-binding regions before a minimal promoter containing a TATA box promoter element and a luciferase reporter gene with low basal activity, which allows sensitive measurement of response-element activity[37]. Cotransfection of those reporter constructs plus a human *Foxp3* expression vector led to significantly less activity for four of the regions with more than one Foxp3-binding motif (**Fig. 4d**). Mutation of the predicted Foxp3-binding motifs in these regions restored the luciferase activity (**Fig. 4d**), which indicated that SATB1 expression was actively repressed by the binding of Foxp3 to several regions in the genomic *SATB1* locus. We derived further support for the idea of Foxp3 binding from *in vitro* DNA-protein–interaction analysis of the binding of recombinant Foxp3 protein to either wild-type or mutated Foxp3-binding motifs; the Foxp3-binding regions BR9 and BR10 demonstrated strong binding of Foxp3 only to the wild-type sequences, whereas the mutated motifs showed almost no interaction with Foxp3 (**Fig. 4e**). Together these data establish Foxp3 as an important repressor that directly binds to the *SATB1* locus in T_{reg} cells and prevents *SATB1* transcription.

Ectopic SATB1 reprograms human T_{reg} cells into T_{eff} cells *in vitro*

To determine whether lower SATB1 expression was required for T_{reg} cells to exert regulatory function, we overexpressed SATB1 in human natural $CD4^+CD25^{hi}$ $Foxp3^+$ T_{reg} cells through the use of a lentiviral vector carrying the *SATB1* full-length transcript (**Supplementary Fig. 8**). We stimulated human T_{reg} cells or T_{conv} cells for 24 h with beads coated with antibody to CD3 (anti-CD3) and anti-CD28 in the presence of IL-2. After stimulating the T_{reg} cells, we transduced them with lentivirus containing a plasmid that expresses the red fluorescent protein DsRED and SATB1 at a ratio of 1:1 (ref. 38) or with a control virus containing a plasmid that expresses only DsRED. We expanded cell populations and then sorted $DsRED^+$ cells. We used only transduced cells with very similar expression of Foxp3 and DsRED for

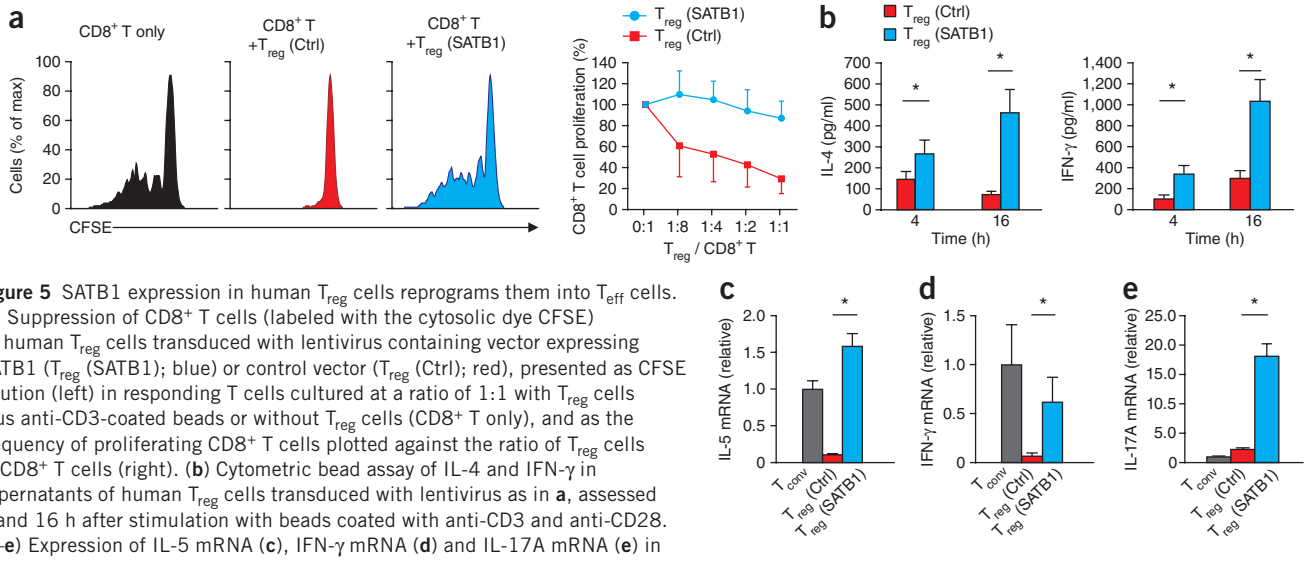

Figure 5 SATB1 expression in human T_{reg} cells reprograms them into T_{eff} cells. (**a**) Suppression of $CD8^+$ T cells (labeled with the cytosolic dye CFSE) by human T_{reg} cells transduced with lentivirus containing vector expressing SATB1 (T_{reg} (SATB1); blue) or control vector (T_{reg} (Ctrl); red), presented as CFSE dilution (left) in responding T cells cultured at a ratio of 1:1 with T_{reg} cells plus anti-CD3-coated beads or without T_{reg} cells ($CD8^+$ T only), and as the frequency of proliferating $CD8^+$ T cells plotted against the ratio of T_{reg} cells to $CD8^+$ T cells (right). (**b**) Cytometric bead assay of IL-4 and IFN-γ in supernatants of human T_{reg} cells transduced with lentivirus as in **a**, assessed 4 and 16 h after stimulation with beads coated with anti-CD3 and anti-CD28. (**c**–**e**) Expression of IL-5 mRNA (**c**), IFN-γ mRNA (**d**) and IL-17A mRNA (**e**) in human T_{conv} cells and T_{reg} cells transduced with lentivirus as in **a** and activated for 16 h with beads as in **b**; results are presented relative to β_2-microglobulin expression. $^*P < 0.05$ (Student's *t*-test). Data are representative of three independent experiments (**a**; mean and s.d.) or are from one experiment representative of two (**b**–**e**; mean and s.d. of triplicate wells), with cells derived from different donors.

further analysis (**Supplementary Fig. 8a**). In contrast to control virus–transduced T_{reg} cells, Foxp3$^+$ T_{reg} cells overexpressing SATB1 lost their suppressive function (**Fig. 5a** and **Supplementary Fig. 8b,c**). At the same time, these cells gained expression of the T_H1 cytokine IFN-γ, the T_H2 cytokine IL-4 and the IL-17-producing helper T cell (T_H17 cell) cytokine IL-17A (**Fig. 5b–e**), which suggested reprogramming of T_{reg} cells into T_{eff} cells in the presence of abundant SATB1 despite their similar Foxp3 expression. As expected, T_{conv} cells transduced with SATB1 by the same approach had no suppressive function (**Supplementary Fig. 9**). These data support the proposal that ectopic expression of SATB1 in T_{reg} cells is sufficient to convert the Foxp3-mediated program into T_{eff} cell programs.

High SATB1 expression induces transcriptional T_{eff} cell programs

To estimate the genome-wide reprogramming in T_{reg} cells overexpressing SATB1, we did whole-transcriptome analysis. Using stringent filter criteria, we found a total of 100 genes with much higher expression in SATB1-expressing T_{reg} cells, whereas 21 had

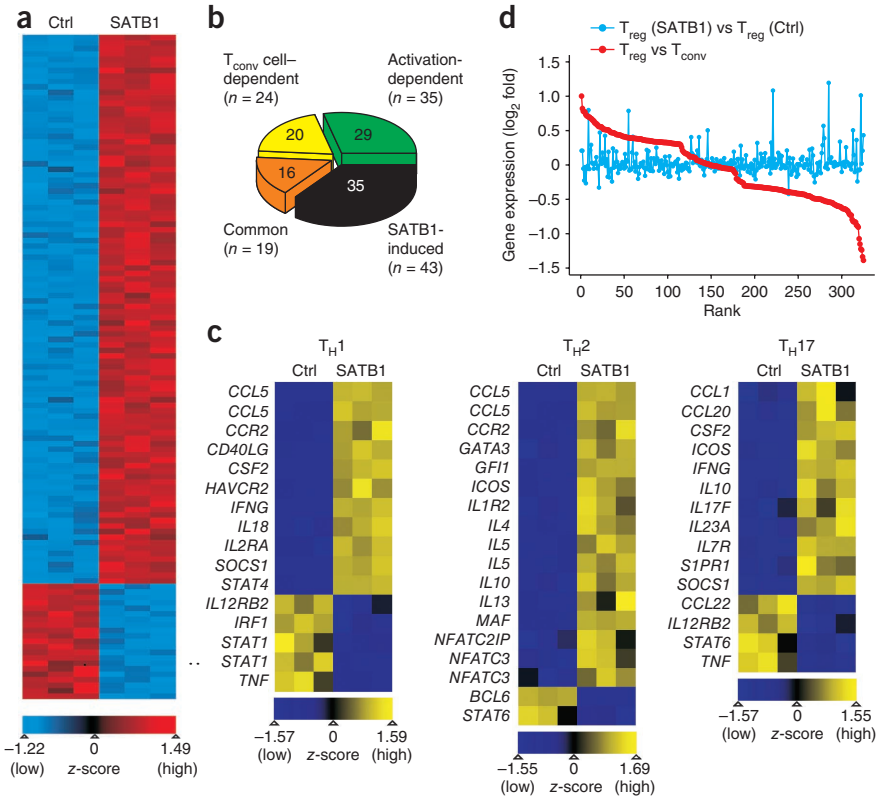

Figure 6 Induction of transcriptional T_{eff} cell programs in SATB1-expressing T_{reg} cells. (**a**) Microarray analysis of human T_{reg} cells transduced with lentivirus containing vector expressing SATB1 (blue) or control vector (red) and stimulated for 16 h with beads coated with anti-CD3 and anti-CD28, presented as a heat map of the *z*-scores of genes with differences in expression. (**b**) Cross-annotation analysis of four classes of genes: those associated with T_{conv} cells but not T_{reg} cells (T_{conv} cell–dependent); those associated with T cell activation (Activation-dependent); common T cell genes (Common); and SATB1-induced genes (SATB1-induced). Numbers in chart indicate percent cells in each group; numbers below labels (*n*) indicate total genes in each group. (**c**) Expression of genes associated with T_H1, T_H2 or T_H17 differentiation, presented as a heat map of *z*-scores. Helper T cell–specific enrichment: T_H1, $P = 3.24 \times 10^{-6}$; T_H2, $P = 9.03 \times 10^{-15}$; T_H17, $P = 1.16 \times 10^{-6}$, versus complete data set (χ^2 test). (**d**) Change in the expression of genes associated with the human T_{reg} cell signature in T_{reg} cells left untransduced (red) or transduced as in **a** (blue), presented as gene expression in T_{reg} cells versus T_{conv} cells or in SATB1-expressing versus control vector–transduced T_{reg} cells, plotted against ranking by change in expression in T_{reg} cells versus T_{conv} cells. Data are from three independent experiments with cells derived from different donors.

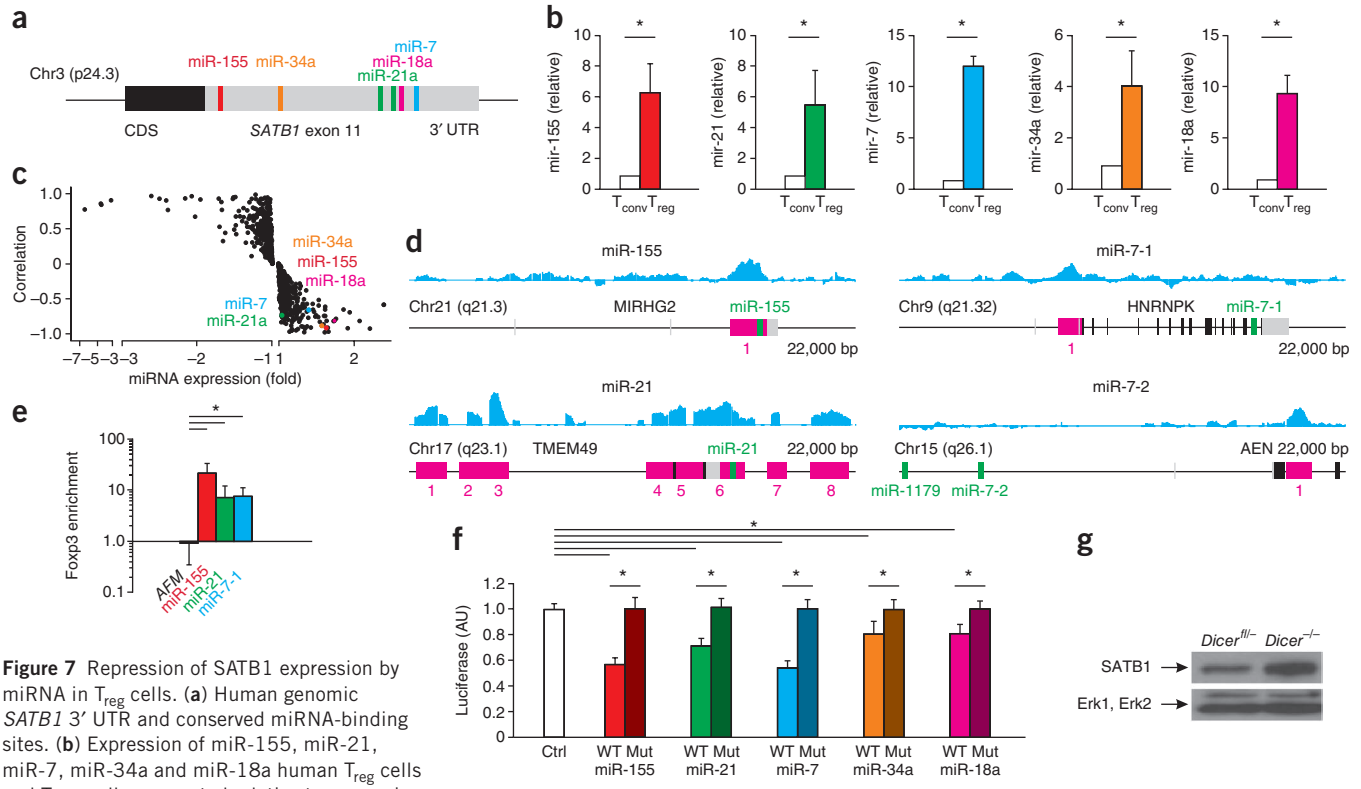

Figure 7 Repression of SATB1 expression by miRNA in T_{reg} cells. (**a**) Human genomic *SATB1* 3′ UTR and conserved miRNA-binding sites. (**b**) Expression of miR-155, miR-21, miR-7, miR-34a and miR-18a human T_{reg} cells and T_{conv} cells, presented relative to expression of the ubiquitously expressed U6 small nuclear RNA. $*P < 0.05$ (Student's *t*-test). (**c**) Correlation of miRNA expression with SATB1 mRNA expression, plotted against change in miRNA expression in T_{reg} cells versus T_{conv} cells, for all 735 miRNAs assessed by microarray (colors for miR-155, miR-21, miR-7, miR-34a and miR-18a correspond to those in **a**,**b**). (**d**) Foxp3 ChIP tiling array data (blue) for miR-155, miR-21 and miR-7-1 and miR-7-2 from expanded populations of human cord blood–derived T_{reg} cells, analyzed by model-based analysis of tiling array and overlaid onto the miRNA locus for identification of binding regions ($P < 10^{-5}$; false-discovery rate <0.5%). (**e**) ChIP analysis of expanded populations of human cord blood–derived T_{reg} cells with a Foxp3-specific antibody and PCR primers specific for miR-155, miR-21 or miR-7-1; results are presented relative to input, normalized to immunoglobulin G. *AFM* (far left), locus encoding α-albumin (negative control). $*P < 0.05$, each miRNA compared with negative control (horizontal lines at top; Student's *t*-test). (**f**) Dual-luciferase assay of HEK293T cells transfected with luciferase constructs containing a wild-type or mutated *SATB1* 3′ UTR (with mutation of the miRNA-responsive elements), together with synthetic mature miRNA or a synthetic control miRNA (Ctrl), presented in arbitrary units (AU) relative to results obtained for control miRNA. $*P < 0.05$ experimental versus control (top) or wild-type versus mutated (directly above bars; Student's *t*-test). (**g**) Immunoblot analysis of SATB1 and Erk1 and Erk2 in T_{reg} cells from mice with complete T_{reg} cell–specific loss of Dicer (*Dicer1*$^{-/-}$) and mice heterozygous for *lox*P-flanked *Dicer* (*Dicer1*$^{fl/-}$). Data are representative of five (**b**) or three (**c**) experiments or two (**d**) or three (**e**) independent experiments with cells derived from different donors, or three (**f**) or two (**g**) independent experiments (mean and s.d. in **b**,**e**,**f**).

lower expression (**Fig. 6a**). Analysis of the genes with differences in expression showed that 20% were associated with higher expression in T_{conv} cells (relative to their expression in T_{reg} cells), 29% of the 'changed' genes were linked mainly with T cell activation and we classified 16% as common T cell genes; the remaining genes (35%) showed no known association with T cell function or lineage, and we classified these as SATB1-induced genes (**Fig. 6b**). Furthermore, compilation of lists of genes associated with T_H1, T_H2 and T_H17 differentiation showed the induction of many genes involved in T_{eff} cell differentiation in SATB1-expressing T_{reg} cells (**Fig. 6c**). In contrast, genes representing the human T_{reg} cell gene signature were unchanged in SATB1-expressing T_{reg} cells (**Fig. 6d**). Because we used polyclonal human T_{reg} cells for this analysis, it was not unexpected that we found the three main T cell–differentiation programs simultaneously. In summary, low SATB1 expression in T_{reg} cells was necessary to permit suppressive function and to ensure inhibition of the effector cell differentiation of T_{reg} cells.

Epigenetic regulation of *SATB1* transcription in T_{reg} cells

The strong dependence of T_{reg} cell function on the repression of *SATB1* indicated the involvement of additional regulatory mechanisms. When assessing DNA methylation, we identified three CpG dinucleotide–rich sites upstream of exon 1 of the *SATB1* locus (**Supplementary Fig. 10**). However, in contrast to the *Foxp3* locus itself[22] (**Supplementary Fig. 10a**), the *SATB1* locus was similarly demethylated in T_{reg} cells and T_{conv} cells (**Supplementary Fig. 10b**), which suggested that DNA methylation does not have a regulatory role at the *SATB1* locus in T_{reg} cells.

Next we examined the chromatin status of the *SATB1* locus by analyzing permissive and repressive histone modifications. ChIP–quantitative PCR of expanded human T_{reg} cell populations showed a lower abundance of permissive trimethylation of histone H3 at Lys4 (**Supplementary Fig. 11a**) and a greater abundance of repressive trimethylation of histone H3 at Lys27 (**Supplementary Fig. 11b**) in human T_{reg} cells than in T_{conv} cells, as well as less acetylation of histone H4 (**Supplementary Fig. 11c**). By assessing a publicly available data set for mouse T_{reg} cells[39], we established the presence of similar histone marks at the mouse *Satb1* locus (**Supplementary Fig. 12**), which suggested that a conserved regulatory circuit exists that contributes to the lower expression of SATB1 in T_{reg} cells by inducing repressive epigenetic marks at the locus encoding SATB1.

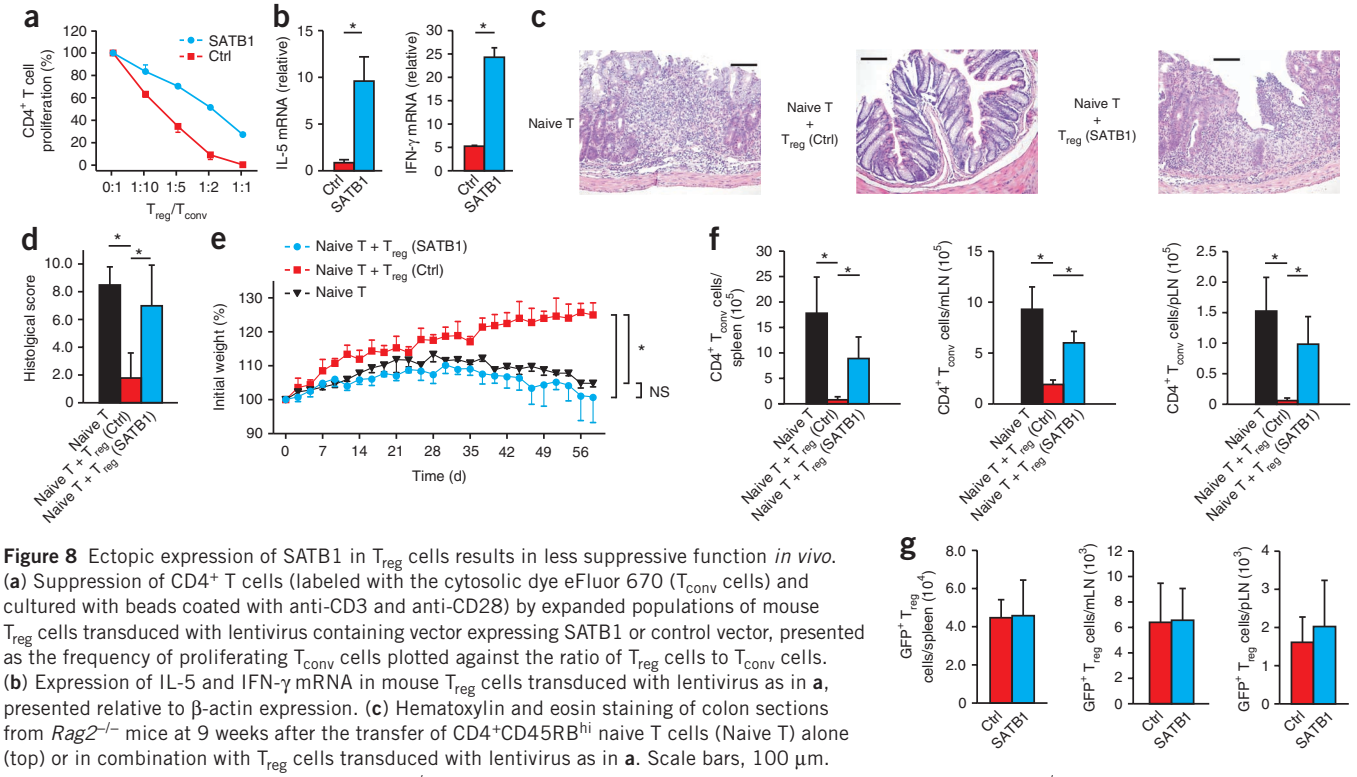

Figure 8 Ectopic expression of SATB1 in T_{reg} cells results in less suppressive function *in vivo*. (**a**) Suppression of CD4$^+$ T cells (labeled with the cytosolic dye eFluor 670 (T_{conv} cells) and cultured with beads coated with anti-CD3 and anti-CD28) by expanded populations of mouse T_{reg} cells transduced with lentivirus containing vector expressing SATB1 or control vector, presented as the frequency of proliferating T_{conv} cells plotted against the ratio of T_{reg} cells to T_{conv} cells. (**b**) Expression of IL-5 and IFN-γ mRNA in mouse T_{reg} cells transduced with lentivirus as in **a**, presented relative to β-actin expression. (**c**) Hematoxylin and eosin staining of colon sections from *Rag2*$^{-/-}$ mice at 9 weeks after the transfer of CD4$^+$CD45RB^{hi} naive T cells (Naive T) alone (top) or in combination with T_{reg} cells transduced with lentivirus as in **a**. Scale bars, 100 μm. (**d**) Histology scores of colon sections of *Rag2*$^{-/-}$ mice at 9 weeks after the cell transfer in **c**. (**e**) Body weight of *Rag2*$^{-/-}$ mice at 9 weeks after the cell transfer in **c**, presented relative to initial body weight. (**f**,**g**) Recovery of T_{conv} cells (**f**) and T_{reg} cells (**g**) from spleens, mesenteric lymph nodes (mLN) and peripheral lymph nodes (pLN) of *Rag2*$^{-/-}$ mice at 9 weeks after the cell transfer in **c**. NS, not significant; $^*P < 0.05$ (Student's *t*-test). Data are representative of two (**a**) or three (**b**) independent experiments (mean and s.e.m. of triplicate cultures (**a**) or mean and s.d. (**b**)) or are pooled from two independent experiments (**c**–**g**; mean and s.d. of four or five recipient mice).

MicroRNAs regulate SATB1 in T_{reg} cells

A prominent layer of post-transcriptional gene regulation is exerted by miRNAs. Profiling of miRNA in human T_{reg} cells and T_{conv} cells allowed us to identify several miRNAs with differences in expression in T_{reg} cells (data not shown). Using inverse correlation analysis of the expression of SATB1 and miRNAs, as well as computational prediction of the binding of miRNA to 'seed-matched' sites (in which only miRNAs matching the canonical sequence of seven to eight nucleotides were used, whereas miRNAs matching marginal sites of six nucleotides were not analyzed as they typically have lower efficacy; **Fig. 7a**), we identified five miRNAs with differences in expression in T_{reg} cells versus T_{conv} cells (**Fig. 7b**) that showed a substantial inverse correlation between SATB1 expression and miRNA expression (**Fig. 7c**). Of those five miRNAs, miR-155, miR-21 and miR-7 were direct targets of Foxp3, as reported before for miR-155 (refs. 31,40,41) and miR-21 (ref. 42) and confirmed by ChIP tiling arrays of Foxp3 and ChIP–quantitative PCR (**Fig. 7d**,**e** and **Supplementary Fig. 13**), as well as functional analysis (S.C.B., unpublished data). Assessment of miRNA expression in T_{conv} cells overexpressing Foxp3 and in T_{reg} cells transfected with siRNA targeting Foxp3 confirmed these miRNAs as targets of Foxp3 (**Supplementary Fig. 14**). To assess functionally relevant binding of the miRNAs to the 3′ untranslated region (UTR) of SATB1 mRNA, we fused the *SATB1* 3′ UTR to a luciferase reporter gene and measured luciferase activity in cells transfected with synthetic miRNAs. Expression of any of the five miRNAs resulted in significant repression of constitutive luciferase activity, with the three miRNAs that were direct targets of Foxp3 showing the greatest effect (**Fig. 7f**). Mutation of the respective binding motifs resulted in restoration of luciferase activity (**Fig. 7f**). As exemplified for miR-155, loss of function of a single miRNA only resulted in minor differences in SATB1 mRNA expression in primary human T_{reg} cells (**Supplementary Fig. 15a**), which indicated that the loss of a single miRNA may be unable to restore SATB1 expression. Complete loss of all miRNAs, however, as achieved in mice by T_{reg} cell–specific deletion of the gene encoding Dicer1 (ref. 21), an endoribonuclease involved in miRNA biogenesis, led to upregulation of SATB1 at the level of both mRNA and protein (**Fig. 7g** and **Supplementary Fig. 15b**). These results suggest that Foxp3 is able to confer T_{reg} cell–specific downregulation of SATB1 expression not only by directly binding to the locus encoding SATB1 but also by inducing a second layer of regulation consisting of miRNAs.

Abundant SATB1 expression results in lower T_{reg} cell function

To assess whether SATB1 expression results in diminished regulatory function of mouse T_{reg} cells *in vitro* and *in vivo*, we overexpressed SATB1 in mouse CD4$^+$ Foxp3$^+$ T_{reg} cells from DEREG mice through the use of a lentivirus encoding the full-length transcript of *Satb1* (**Supplementary Fig. 16**). We sorted CD4$^+$ Foxp3$^+$ T_{reg} cells from DEREG mice and expanded the cell populations for 10–14 d with beads coated with anti-CD3 and anti-CD28 in the presence of IL-2. After that initial expansion period, we transduced the expanded T_{reg} cell populations with lentivirus containing a plasmid encoding SATB1, an internal ribosomal entry site and the alloantigen Thy-1.1 or control lentivirus containing a plasmid encoding Thy-1.1 alone. We expanded cell populations for 4 additional days in the presence of beads coated with anti-CD3 and anti-CD28 and IL-2 before sorting Thy-1.1$^+$ GFP$^+$ T_{reg} cells. T_{reg} cells transduced with SATB1-expressing

or control lentivirus had similar Foxp3 expression (**Supplementary Fig. 16a**). In contrast to control lentivirus–transduced T_{reg} cells, Foxp3$^+$ T_{reg} cells overexpressing SATB1 showed loss of suppressive function and acquisition of the expression of the effector cytokines IFN-γ (T_H1) and IL-5 (T_H2; **Fig. 8a**,**b** and **Supplementary Fig. 16b**–**f**), which supported the idea of the reprogramming of T_{reg} cells into T_{eff} cells in the presence of high SATB1 expression.

To assess *in vivo* suppressor capacity of the manipulated T_{reg} cells, we transferred control T_{reg} cells or SATB1-overexpressing T_{reg} cells together with naive CD4$^+$CD45RB^{hi} T cells (isolated from normal mice) into recipient mice deficient in recombination-activating gene 2 (*Rag2*$^{-/-}$ mice). Transfer of naive CD4$^+$CD45RB^{hi} T cells alone led to the development of colitis (**Fig. 8c**–**e**). As expected, *Rag2*$^{-/-}$ mice that received naive CD4$^+$CD45RB^{hi} T cells and control T_{reg} cells did not develop colitis-associated pathology (**Fig. 8c**–**e**), whereas mice that received only naive CD4$^+$CD45RB^{hi} cells had colonic infiltrates and weight loss. Transfer of SATB1-overexpressing T_{reg} cells together with naive CD4$^+$CD45RB^{hi} T cells resulted in colitis-associated pathology (**Fig. 8c**–**e**), which suggested impairment of the suppressor function of SATB1-overexpressing T_{reg} cells with a concomitant gain of effector function. We observed significant expansion of the number of T_{conv} cells in spleen, mesenteric and peripheral lymph nodes of mice that received either no T_{reg} cells or SATB1-overexpressing T_{reg} cells (**Fig. 8f**), whereas the number of cells that maintained Foxp3 expression in spleen, mesenteric and peripheral lymph nodes was equal in mice that received control or SATB1-overexpressing T_{reg} cells (**Fig. 8g**). Thus, Foxp3$^+$ T_{reg} cells with high expression of SATB1 showed less suppressor function with a concomitant gain of T_{eff} cell programs *in vivo* and *in vitro*, which suggested that downregulation of SATB1 in T_{reg} cells was necessary for the maintenance of a stable suppressive phenotype (**Supplementary Fig. 17**).

DISCUSSION

For T_{reg} cells, many mechanisms have been linked to their suppressive function after contact with other effector cells of the immune response[1]. However, intrinsic inhibition of T_{eff} cell function mainly by Foxp3-induced mechanisms seems to be necessary for T_{reg} cells to exert suppressive function. In this report we have shown that repression of SATB1 in T_{reg} cells was required for the suppressive function and inhibition of effector differentiation of these cells. As upregulation of SATB1 was required for the induction of T_{eff} cell cytokines in T_{conv} cells the profound lack of upregulation of SATB1 after stimulation of T_{reg} cells suggested that Foxp3-mediated suppression of SATB1 has an important role in inhibiting cytokine production in T_{reg} cells. In support of that proposal, high ectopic expression of SATB1 in T_{reg} cells led to the induction of T_{eff} cell cytokines and loss of suppressive function despite the expression of Foxp3 *in vitro* and *in vivo*. Mechanistically, SATB1 expression was controlled directly by Foxp3-mediated transcriptional repression and histone modification, as well as by induction of the binding of miRNA to the 3′ UTR of SATB1. Together these findings establish that the continuous active repression of central mechanisms involved in T_{eff} cell programs provided by SATB1 is necessary for T_{reg} cells to exert their suppressive function.

Thus, a major finding of our study is that T_{reg} cells depended not only on the induction of Foxp3-mediated genes associated with suppressive function but also on the specific repression of molecules such as SATB1 to prevent T_{eff} cell function. Low SATB1 expression seems to be necessary for retention of functional T cell integrity not only in T_{conv} cells but also in T_{reg} cells, as mice completely deficient in SATB1 are basically devoid of T cells in the periphery[25]. Although Foxp3 dictates the repression of SATB1 in T_{reg} cells, thereby preventing T_{eff} cell function, we have no evidence so far for inverse control of Foxp3 by SATB1 in T_{conv} cells; together these findings favor a model in which T_{eff} cell programs are continually and actively over-ruled by Foxp3-mediated transcriptional repression in T_{reg} cells.

Further evidence for such a model has been provided by studies elucidating the effect of the transcriptional repressor Eos on T_{reg} cells[13]. Eos directly interacts with Foxp3 to specifically induce chromatin modifications that result in gene silencing, whereas genes induced by Foxp3 are not affected. Notably, loss of Eos abrogates suppressive T_{reg} cell function but only partially endows T_{reg} cells with T_{eff} cell functions, consistent with the normal repression of T_{eff} cell differentiation in T_{reg} cells. Similarly, loss of Runx1-CBFβ heterodimers, another component of the multiprotein complex that contains Foxp3, in T_{reg} cells leads to lower Foxp3 expression, loss of suppressor function and gain of IL-4 expression by T_{reg} cells[43,44]. Foxp3, as well as Eos and Runx1-CBFβ heterodimers, have been shown to directly repress certain effector cytokines, such as IFN-γ or IL-4, which suggests that T_{reg} cells may use multiple mechanisms to suppress T_{eff} cell programs[13,18,43]. Nevertheless, ectopic expression of SATB1 in T_{reg} cells was sufficient to induce effector cytokines, which suggests that large amounts of SATB1 can overcome the repression of downstream targets by Foxp3. This might be similarly true in activated T_{conv} cells that have lower expression of Foxp3 temporarily during early activation phases.

The transcription factors Foxo1 and Foxo3 have also been linked to the inhibition of T_{eff} cell function in T_{reg} cells[14]. Notably, lack of Foxo1 and Foxo3 in T_{reg} cells is sufficient to induce T_H1 and T_H17 effector cytokines but not T_H2 cytokines, whereas SATB1 seems to have a more profound effect on T_H2 cytokines under certain conditions[29,45]. Together these findings point to a hierarchy of repressive mechanisms that ensure suppression of T_{eff} cell function in T_{reg} cells. Our findings support a model of continuously active regulatory networks that shape the overall function of T cells in the periphery as an alternative to terminal differentiation. Active and continuous blockade of T_{eff} cell function instead of terminal T_{reg} cell differentiation allows T cells a greater degree of functional plasticity, such as under inflammatory conditions in which T_{reg} cells can gain effector function once Foxp3 is switched off[24,46–48].

METHODS

Methods and any associated references are available in the online version of the paper at http://www.nature.com/natureimmunology/.

Accession codes. GEO: microarray data, GSE15390; tiling array data, GSE20995.

Note: Supplementary information is available on the Nature Immunology website.

ACKNOWLEDGMENTS

We thank M. Mai, M. Kraut, S. Keller, N. Kuhn, J. Birke, I. Büchmann, A. Dolf and P. Wurst for technical assistance; M. Hoch, M. Pankratz, S. Burgdorf, A. Popov and A. Staratschek-Jox, as well as all other laboratory members, for discussions; and J. Oldenburg for blood samples from healthy subjects. Supported by the German Research Foundation (Sonderforschungsbereich 832, SFB 704, INST 217/576-1 and INST 217/577-1 to J.L.S. and M.B.), the Wilhelm-Sander-Foundation (J.L.S. and M.B.), the German Cancer Aid (J.L.S.), the German Jose-Carreras-Foundation (J.L.S. and M.B.), the Federal Ministry of Education and Research (Nationale Genomforschungsnetz 2 to J.L.S.), the Humboldt Foundation (J.L.S.), the Leukemia and Lymphoma Society of America (R6029-07 to B.R.B. and K.L.H.), the Juvenile Diabetes Research Foundation (16-2008-643 to X.Z., S.L.B.-B. and J.A.B.), the University of California, San Francisco, Autoimmunity Center of Excellence (X.Z., S.L.B.-B. and J.A.B.), the National Health and Medical Research Council (339123, 565314 to S.C.B.), the German Research Foundation (SCHE 1562 and

SFB832 to B.S.), the Juvenile Diabetes Research Foundation Collaborative Centers for Cell Therapy (S.B., T.G. and J.L.R.) and the Juvenile Diabetes Research Foundation Center on Cord Blood Therapies for Type 1 Diabetes (S.B., T.G. and J.L.R.).

AUTHOR CONTRIBUTIONS

M.B. designed, did and supervised experiments, analyzed data and wrote the manuscript; Y.T. did quantitative PCR, cytometric bead assay, immunoblot analysis, overexpression experiments and filter-retention analysis and analyzed data; R.-U.M. designed and did reporter assays; S.C. did experiments and analyzed data; T.S. did ChIP experiments and analyzed data; K.L. and C.T.M. did experiments with DEREG mice; S.B. and T.G. did overexpression experiments; E.A.S. did and analyzed immunofluorescence experiments; W.K. did histone-methylation studies, S.L.B.-B. and X.Z. did experiments with mice with *lox*P-flanked *Dicer1* alleles; A.H. did bioinformatics analysis; D.S. generated lentivirus contructs; S.D.-P. did microarray experiments; E.E. did flow cytometry sorting; J.B. and A.L. did experiments with *Rag2*$^{-/-}$ mice; P.A.K. was involved in study design; K.L.H. and B.R.B. provided vital analytical tools; R.B. provided vital analytical tools; T.Q. supervised and analyzed immunofluorescence experiments; C.W. did immunohistochemistry; A.W. did, designed and supervised DNA-methylation experiments; G.M. and M.F. designed and supervised filter-retention experiments; W.K. designed and supervised experiments and wrote the manuscript; B.S. designed and analyzed reporter assays; S.C.B. designed and supervised ChIP experiments; T.S. designed and supervised experiments with DEREG mice and provided vital analytical tools; J.A.B. designed and supervised experiments with mice with *lox*P-flanked *Dicer1* alleles; J.L.R. designed and supervised SATB1-overexpression experiments and wrote the manuscript; J.L.S. designed, supervised and analyzed experiments and wrote the manuscript; and all authors discussed the results and commented on the manuscript.

COMPETING FINANCIAL INTERESTS

The authors declare competing financial interests: details accompany the full-text HTML version of the paper at http://www.nature.com/natureimmunology/.

Published online at http://www.nature.com/natureimmunology/.
Reprints and permissions information is available online at http://www.nature.com/reprints/index.html.

1. Sakaguchi, S., Yamaguchi, T., Nomura, T. & Ono, M. Regulatory T cells and immune tolerance. *Cell* **133**, 775–787 (2008).
2. Lin, W. *et al.* Regulatory T cell development in the absence of functional Foxp3. *Nat. Immunol.* **8**, 359–368 (2007).
3. Wan, Y.Y. & Flavell, R.A. Regulatory T-cell functions are subverted and converted owing to attenuated Foxp3 expression. *Nature* **445**, 766–770 (2007).
4. Lahl, K. *et al.* Nonfunctional regulatory T cells and defective control of Th2 cytokine production in natural scurfy mutant mice. *J. Immunol.* **183**, 5662–5672 (2009).
5. Williams, L.M. & Rudensky, A.Y. Maintenance of the Foxp3-dependent developmental program in mature regulatory T cells requires continued expression of Foxp3. *Nat. Immunol.* **8**, 277–284 (2007).
6. Fontenot, J.D., Gavin, M.A. & Rudensky, A.Y. Foxp3 programs the development and function of CD4$^+$CD25$^+$ regulatory T cells. *Nat. Immunol.* **4**, 330–336 (2003).
7. Hori, S., Nomura, T. & Sakaguchi, S. Control of regulatory T cell development by the transcription factor Foxp3. *Science* **299**, 1057–1061 (2003).
8. O'Shea, J.J. & Paul, W.E. Mechanisms underlying lineage commitment and plasticity of helper CD4v T cells. *Science* **327**, 1098–1102 (2010).
9. Murphy, K.M. & Stockinger, B. Effector T cell plasticity: flexibility in the face of changing circumstances. *Nat. Immunol.* **11**, 674–680 (2010).
10. Feuerer, M., Hill, J.A., Mathis, D. & Benoist, C. Foxp3$^+$ regulatory T cells: differentiation, specification, subphenotypes. *Nat. Immunol.* **10**, 689–695 (2009).
11. Lee, Y.K., Mukasa, R., Hatton, R.D. & Weaver, C.T. Developmental plasticity of Th17 and Treg cells. *Curr. Opin. Immunol.* **21**, 274–280 (2009).
12. Gavin, M.A. *et al.* Foxp3-dependent programme of regulatory T-cell differentiation. *Nature* **445**, 771–775 (2007).
13. Pan, F. *et al.* Eos mediates Foxp3-dependent gene silencing in CD4$^+$ regulatory T cells. *Science* **325**, 1142–1146 (2009).
14. Ouyang, W. *et al.* Foxo proteins cooperatively control the differentiation of Foxp3$^+$ regulatory T cells. *Nat. Immunol.* **11**, 618–627 (2010).
15. Harada, Y. *et al.* Transcription factors Foxo3a and Foxo1 couple the E3 ligase Cbl-b to the induction of Foxp3 expression in induced regulatory T cells. *J. Exp. Med.* **207**, 1381–1391 (2010).
16. Zheng, Y. *et al.* Regulatory T-cell suppressor program co-opts transcription factor IRF4 to control T_H2 responses. *Nature* **458**, 351–356 (2009).
17. Chaudhry, A. *et al.* CD4$^+$ regulatory T cells control T_H17 responses in a Stat3-dependent manner. *Science* **326**, 986–991 (2009).
18. Ziegler, S.F. FOXP3: of mice and men. *Annu. Rev. Immunol.* **24**, 209–226 (2006).
19. Chong, M.M., Rasmussen, J.P., Rudensky, A.Y. & Littman, D.R. The RNAseIII enzyme Drosha is critical in T cells for preventing lethal inflammatory disease. *J. Exp. Med.* **205**, 2005–2017 (2008).
20. Liston, A., Lu, L.F., O'Carroll, D., Tarakhovsky, A. & Rudensky, A.Y. Dicer-dependent microRNA pathway safeguards regulatory T cell function. *J. Exp. Med.* **205**, 1993–2004 (2008).
21. Zhou, X. *et al.* Selective miRNA disruption in T reg cells leads to uncontrolled autoimmunity. *J. Exp. Med.* **205**, 1983–1991 (2008).
22. Floess, S. *et al.* Epigenetic control of the foxp3 locus in regulatory T cells. *PLoS Biol.* **5**, e38 (2007).
23. Li, B. *et al.* FOXP3 interactions with histone acetyltransferase and class II histone deacetylases are required for repression. *Proc. Natl. Acad. Sci. USA* **104**, 4571–4576 (2007).
24. Zhou, X., Bailey-Bucktrout, S., Jeker, L.T. & Bluestone, J.A. Plasticity of CD4$^+$ FoxP3$^+$ T cells. *Curr. Opin. Immunol.* **21**, 281–285 (2009).
25. Alvarez, J.D. *et al.* The MAR-binding protein SATB1 orchestrates temporal and spatial expression of multiple genes during T-cell development. *Genes Dev.* **14**, 521–535 (2000).
26. Cai, S., Han, H.J. & Kohwi-Shigematsu, T. Tissue-specific nuclear architecture and gene expression regulated by SATB1. *Nat. Genet.* **34**, 42–51 (2003).
27. Yasui, D., Miyano, M., Cai, S., Varga-Weisz, P. & Kohwi-Shigematsu, T. SATB1 targets chromatin remodelling to regulate genes over long distances. *Nature* **419**, 641–645 (2002).
28. Dickinson, L.A., Joh, T., Kohwi, Y. & Kohwi-Shigematsu, T. A tissue-specific MAR/SAR DNA-binding protein with unusual binding site recognition. *Cell* **70**, 631–645 (1992).
29. Cai, S., Lee, C.C. & Kohwi-Shigematsu, T. SATB1 packages densely looped, transcriptionally active chromatin for coordinated expression of cytokine genes. *Nat. Genet.* **38**, 1278–1288 (2006).
30. Pfoertner, S. *et al.* Signatures of human regulatory T cells: an encounter with old friends and new players. *Genome Biol.* **7**, R54 (2006).
31. Zheng, Y. *et al.* Genome-wide analysis of Foxp3 target genes in developing and mature regulatory T cells. *Nature* **445**, 936–940 (2007).
32. Sugimoto, N. *et al.* Foxp3-dependent and -independent molecules specific for CD25$^+$CD4$^+$ natural regulatory T cells revealed by DNA microarray analysis. *Int. Immunol.* **18**, 1197–1209 (2006).
33. Lund, R. *et al.* Identification of genes involved in the initiation of human Th1 or Th2 cell commitment. *Eur. J. Immunol.* **35**, 3307–3319 (2005).
34. Chen, W. *et al.* Conversion of peripheral CD4$^+$CD25$^-$ naive T cells to CD4$^+$CD25$^+$ regulatory T cells by TGF-beta induction of transcription factor Foxp3. *J. Exp. Med.* **198**, 1875–1886 (2003).
35. Lahl, K. *et al.* Selective depletion of Foxp3$^+$ regulatory T cells induces a scurfy-like disease. *J. Exp. Med.* **204**, 57–63 (2007).
36. Kuczma, M. *et al.* Foxp3-deficient regulatory T cells do not revert into conventional effector CD4$^+$ T cells but constitute a unique cell subset. *J. Immunol.* **183**, 3731–3741 (2009).
37. Ishihara, Y., Ito, F. & Shimamoto, N. Increased expression of c-Fos by extracellular signal-regulated kinase activation under sustained oxidative stress elicits BimEL upregulation and hepatocyte apoptosis. *FEBS J.* **278**, 1873–1881 (2011).
38. Szymczak, A.L. *et al.* Correction of multi-gene deficiency *in vivo* using a single 'self-cleaving' 2A peptide-based retroviral vector. *Nat. Biotechnol.* **22**, 589–594 (2004).
39. Wei, G. *et al.* Global mapping of H3K4me3 and H3K27me3 reveals specificity and plasticity in lineage fate determination of differentiating CD4+ T cells. *Immunity* **30**, 155–167 (2009).
40. Lu, L.F. *et al.* Foxp3-dependent microRNA155 confers competitive fitness to regulatory T cells by targeting SOCS1 protein. *Immunity* **30**, 80–91 (2009).
41. Kohlhaas, S. *et al.* Cutting edge: the Foxp3 target miR-155 contributes to the development of regulatory T cells. *J. Immunol.* **182**, 2578–2582 (2009).
42. Marson, A. *et al.* Foxp3 occupancy and regulation of key target genes during T-cell stimulation. *Nature* **445**, 931–935 (2007).
43. Kitoh, A. *et al.* Indispensable role of the Runx1-Cbfβ transcription complex for *in vivo*-suppressive function of FoxP3$^+$ regulatory T cells. *Immunity* **31**, 609–620 (2009).
44. Rudra, D. *et al.* Runx-CBFβ complexes control expression of the transcription factor Foxp3 in regulatory T cells. *Nat. Immunol.* **10**, 1170–1177 (2009).
45. Ahlfors, H. *et al.* SATB1 dictates expression of multiple genes including IL-5 involved in human T helper cell differentiation. *Blood* **116**, 1443–1453 (2010).
46. Koch, M.A. *et al.* The transcription factor T-bet controls regulatory T cell homeostasis and function during type 1 inflammation. *Nat. Immunol.* **10**, 595–602 (2009).
47. Zhou, X. *et al.* Instability of the transcription factor Foxp3 leads to the generation of pathogenic memory T cells *in vivo*. *Nat. Immunol.* **10**, 1000–1007 (2009).
48. Oldenhove, G. *et al.* Decrease of Foxp3$^+$ Treg cell number and acquisition of effector cell phenotype during lethal infection. *Immunity* **31**, 772–786 (2009).

ONLINE METHODS

Mice. DEREG mice, scurfy mice, DEREG × scurfy mice, Foxp3-GFP-hCre BAC × *Dicer1*$^{fl/fl}$ mice and Foxp3-GFP-hCre BAC × *Dicer1*$^{fl/fl}$ × ROSA26R-YFP mice have been described[4,21,35,49]. All animal experiments were approved by the relevant Institutional Animal Care and Use Committee (University of California, San Francisco; Lower Saxony, Germany; or North Rhine Westfalia, Germany).

Antibodies and flow cytometry. Fluorescent dye–conjugated antibodies were from Becton Dickinson, BioLegend or eBioscience. Alexa Fluor 647–conjugated mouse monoclonal antibody to human SATB1 (14) cross-reactive to mouse SATB1 was prepared by R. Balderas (Becton Dickinson Biosciences). The FOXP3 Fix/Perm Buffer Set (BioLegend) was used for intracellular staining of human and mouse Foxp3 and SATB1.

Purification and sorting of human T_{reg} cells. Human T_{reg} cells and T_{eff} cells were purified from the whole blood of healthy human donors in compliance with Institutional Review Board protocols (ethics committee of the University of Bonn) by negative selection with the RosetteSep Human CD4 Depletion Cocktail (Stem Cell), followed by positive selection with CD25-specific MACS beads (Miltenyi Biotech) or sorting on a FACSDiva or FACSAria III (both from BD) after incubation of cells with combinations of fluorochrome-labeled monoclonal anti-CD4 (RPA-T4), anti-CD25 (M-A251) and anti-CD127 (hIL-7R-M21; all from BD).

Quantitative RT–PCR. Total RNA extracted with TRIzol (Invitrogen) was used for the generation of cDNA along with the Transcriptor First Strand cDNA Synthesis Kit (Roche Diagnostics). A LightCycler Taqman Master Kit and a Universal Probe Library assay on a LightCycler 480 II (Roche Diagnostics) were used for quantitative RT-PCR (primer sequences, **Supplementary Tables 3** and **4**). Results were normalized to the expression of β_2-microglobulin for human samples or β-actin for mouse samples.

Immunoblot analysis. Lysates of purified cells were prepared as described[50], followed by immunoblot analysis with anti-SATB1 (14; BD) and antibody to human β-actin (C4; Millipore) or antibody to mouse Erk1 and Erk2 (L34F12; Cell Signaling) as a loading control.

Whole-genome gene expression in human cells. RNA was extracted with TRIzol (Invitrogen) and purified by standard methods. Sample amplification, labeling and hybridization on HumanWG-6 v1 or v3 Expression BeadChip arrays were done for all arrays according to the manufacturer's instructions (Illumina). All data were analyzed with Bioconductor software (for the analysis and comprehension of high-throughput genomic data) of the R project for statistical computing.

Immunofluorescence microscopy. Unpurified lymphocytes from male DEREG mice or CD4$^+$ GFP$^+$ T_{reg} cells from female heterozygous DEREG × scurfy mice, purified from the thymus, were fixed for 10 min in cold paraformaldehyde, washed with PBS, made permeable with Triton-X and preblocked for 30 min in PBS containing 10% (vol/vol) normal goat serum and 1% (vol/vol) gelatine from the skin of coldwater fish. Slides were then incubated for 60 min with combinations of primary antibodies (rabbit anti-GFP; A11122; Invitrogen), mouse anti-Foxp3 (eBio7979; eBioscience), Alexa Fluor 647–conjugated mouse anti-SATB1 (14; BD Biosciences)) and washed twice and then incubated for 60 min with secondary antibodies (Alexa Fluor 488–conjugated goat antibody to rabbit immunoglobulin G (IgG; A11034) or Alexa Fluor 555–conjugated goat antibody to mouse IgG (A21422; both from Invitrogen)) and stained with DAPI (4,6-diamidino-2-phenylindole), and fluorescence was examined with an Olympus FluoView FV1000 or Zeiss LSM 5 LIVE confocal microscope.

ChIP, whole-genome arrays and ChIP–quantitative PCR. Expanded populations of human cord blood T_{reg} cells were cultured overnight and then stimulated with ionomycin, then crosslinked for 10 min in 1% (vol/vol) formaldehyde solution. Cell lysis, ChIP and DNA isolation, as well as data acquisition and analysis of human Foxp3 by ChIP plus micrarray, were done as described[51].

The binding of Foxp3 to genomic regions was confirmed by ChIP–quantitative PCR (primer sequences, **Supplementary Table 5**) with RT2 SYBRgreen/ROX qPCR Master Mix (SABiosciences). The enrichment of target regions in the products of immunoprecipitation with rabbit IgG anti-Foxp3 (NB600-245; Novus Biologicals) relative to input chromatin was calculated by change in cycling threshold ($2^{-\Delta\Delta CT}$ method). Immunoprecipitation with ChIP-grade control rabbit IgG (ab46540; Abcam) was used to normalize for nonspecific background.

Gene-specific mRNA silencing, miRNA knockdown and agonistic miRNA. All siRNA as well as the miRNA mimics and inhibitors were from Biomers or Dharmacon. The miRNA mimics were designed according to sequences published in the miRBase searchable database of published miRNA sequences and annotation resembling the double-stranded products of Dicer cleavage (sequences, **Supplementary Tables 6** and **7**). Inhibitors of miRNA were designed as single-stranded antisense 2-O-methyl oligonucleotides. Those were used for transfection of freshly isolated primary human T_{reg} cells by nucleofection. For luciferase assays, HEK293T cells were transfected with both reporter plasmids and small RNA duplexes through the use of Lipofectamine 2000 in a 96-well format and luciferase activity was measured 24 h later.

Profiling and quantitative RT–PCR of miRNA. All RNA was extracted with TRIzol (Invitrogen) and purified by standard methods. Sample amplification, labeling and hybridization on an Illumina MicroRNA Universal Array Matrix were done with a human v1 MicroRNA Expression Profiling kit for all arrays in this study according to the manufacturer's instructions (Illumina) with an Illumina BeadStation. All data were analyzed with Bioconductor for the R project. For miRNA-specific quantitative RT-PCR, total RNA was extracted with TRIzol. First-strand cDNA for each miRNA was synthesized with a TaqMan MicroRNA Reverse Transcription kit and the corresponding miRNA-specific kit (Applied Biosystems). The abundance of miRNA was measured by quantitative PCR with the TaqMan Universal PCR Master Mix (Applied Biosystems) on a LightCycler 480 II (Roche Diagnostics). Ubiquitously expressed U6 small nuclear RNA was used for normalization.

Cloning of *SATB1* 3′ UTR constructs. The *SATB1* 3′ UTR was amplified by PCR with human genomic DNA as the source material. The full-length 3′ UTR construct was amplified with primers covering the full 1.2-kilobase region (sequences, **Supplementary Table 8**). After digestion with XhoI and NotI, the fragment was cloned into the vector psiCHECK II (Promega) to generate psiCHECK II–*SATB1*–3′UTR. A mutated construct was generated by PCR-based mutagenesis or the QuikChange Lightning Multi Site-Directed mutagenesis kit according to the manufacturer's conditions (sequences, **Supplementary Table 9**; Stratagene). Binding sites for miRNA were altered by 'swapping' of four nucleotides in the seed region (sequences, **Supplementary Table 10**).

Cloning of *SATB1* constructs with potential Foxp3-binding regions. *SATB1* genomic regions were amplified by PCR with human genomic DNA as the source material (sequences, **Supplementary Table 11**). After digestion, the potential binding motifs were cloned into the pGL4.24 vector before a minimal promoter containing a TATA box promoter element and a destabilized firefly luciferase reporter gene with low basal activity, which allows sensitive measurement of response element activity. Mutated constructs of the potential binding motifs (sequences, **Supplementary Table 12**) were generated by either PCR-based mutagenesis or the QuikChange Lightning Multi Site-Directed mutagenesis kit according to the manufacturer's conditions (sequences, **Supplementary Table 13**; Stratagene).

Luciferase assay. For analysis of the regulation of SATB1 expression by the binding of miRNA to the 3′ UTR of *SATB1*, constructs were transfected into HEK293T cells in 96-well plates together with miRNA mimics for miR-155, miR-7, miR-21, miR-34a or miR-18a or a scrambled control miRNA. For analysis of the regulation of SATB1 expression by the binding of Foxp3 to the genomic locus of *SATB1*, constructs were transfected separately into HEK293T cells in 96-well plates together with control plasmid or plasmid expressing Foxp3, as well as a plasmid encoding renilla luciferase for normalization.

doi:10.1038/ni.2084

Lysis and analysis were done 24 h after transfection with a Dual Luciferase Kit (Promega). Luciferase activity was measured with a Mithras plate reader (Berthold).

Lentivirus production. Supernatants with a high titer of lentivirus vector encoding DsRED T2A SATB1 or YFP T2A Foxp3 or control plasmid alone were collected. For silencing of *FOXP3* and *SATB1* in human T_{reg} cells, miRNA targeting these genes for RNA-mediated interference was designed (oligonucleotide sequences, **Supplementary Table 14**), cloned into the pcDNA6.2-GW+EmGFP-miR vector, 'chained' and recombined into pLenti6.3 expression vectors (Invitrogen). For transduction of expanded populations of mouse T_{reg} cells, *Satb1* was cloned into the pLVTHM expression vector before an internal ribosomal entry site–Thy-1.1 sequence[52].

Transduction of human CD4$^+$ T cells with lentivirus expressing Foxp3 and SATB1. Human CD4$^+$CD25$^+$ T_{reg} cells were stimulated for 24 h with beads coated with anti-CD3 and anti-CD28 in the presence of IL-2. After that initial stimulation, the cells were transduced with lentivirus containing the plasmid pELNS DsRED 2A SATB1 or control plasmid encoding DsRED alone, as described, which resulted in 1:1 expression of DsRED and the transgene[38]. Cell populations were expanded for 6 d in the presence of beads coated with anti-CD3 and anti-CD28 plus IL-2, followed by sorting of DsRED$^+$ cells on a MoFlo sorter (DakoCytomation) and use in further experiments.

Bisulphite sequencing. Genomic DNA from human T_{reg} cells and conventional T cells was isolated by phenol-chloroform extraction. Genomic DNA was treated with sodium bisulphate, which resulted in the deamination of unmethylated cytosines to uracil, whereas methylated cytosines remain unchanged. After amplification, PCR products were purified and sequenced in both directions (primer sequences, **Supplementary Table 15**).

Filter-retention analysis. Each individual ^{32}P-radiolabeled double-stranded DNA sequence (14 nM; oligonucleotide sequences, **Supplementary Table 16**) was incubated for 30 min at 37 °C with increasing concentrations of Foxp3 protein in 25 μl binding buffer (KCl-Tris, pH 7.6, 5% (vol/vol) glycerol, 3 mM $MgCl_2$ and 2 mM dithiothreitol) in the presence of transfer RNA (1 μg/ml; Roche) and BSA (50 μg/ml). After that incubation, the binding reaction was filtered through pre-wet 0.45-μm nitrocellulose filter membrane (Millipore) for retention of both protein and bound DNA. Membranes were washed and bound DNA-protein complexes were quantified by autoradiography.

Population expansion of mouse T_{reg} cells. CD4$^+$CD25$^+$GFP$^+$ T_{reg} cells were isolated from lymph nodes and spleens of DEREG mice. Cells were pre-enriched with a Mouse CD4$^+$ T cell Isolation Kit II according to the manufacturer's instructions (Miltenyi Biotech). After enrichment, cells were stained with anti-CD4 (RM4-5), anti-CD25 (PC61), anti-CD3 (500A2) and anti-CD8α (53-6.7; all from BD). Cells were sorted on a FACSAria III (BD) to a purity of >98.0%. Cell populations were expanded *in vitro* by activation with Dynabead mouse T-Activator microbeads coated with anti-CD3 and anti-CD28 (bead/T_{reg} cell ratio, 3:1; Invitrogen) plus exogenous IL-2 (2,000 IU/ml; Proleukin) as described[53].

Transduction of mouse T_{reg} cells with lentivirus. After population expansion for 10–14 d in the presence of beads coated with anti-CD3 and anti-CD28 plus IL-2, mouse T_{reg} cells (2.5×10^5 cells per well) were transduced with lentivirus containing a pLVTHM-SATB1-IRES-Thy-1.1 plasmid or control plasmid, in 500 μl total volume of fresh culture medium in a 24-well plate containing lentivirus (multiplicity of infection, 40) and protamine sulfate (8 μg/ml; Sigma-Aldrich). Cells were spin-inoculated by centrifugation at 1,000*g* for 90 min at 30 °C, then fresh medium was added and cells were incubated for an additional 2 h at 37 °C. Afterward, cells were washed several times and cultivated in the presence of beads coated with anti-CD3 and anti-CD28 plus IL-2. Transgene expression was assessed no earlier than 72 h after transduction. Expanded populations of T_{reg} cells left untransduced or transduced with lentivirus containing the plasmid expressing SATB1 and Thy-1.1 or control plasmid were sorted on a FACSAria III (BD) on the basis of their expression of GFP and Thy-1.1 or GFP expression alone and were used for further experiments.

Induction and assessment of colitis. Splenocyte samples were enriched for CD4$^+$ T cells by negative selection with a Mouse CD4$^+$ T cell Isolation Kit II (Miltenyi Biotec). Cells were then stained with anti-CD45RB (16A), anti-CD25 (PC61), anti-CD4 (RM4-5), anti-CD8α (53-6.7) and anti-CD3 (500A2; all from BD), and naive CD4$^+$CD25$^-$CD45RB^{hi} T cells were sorted on a FACSAria III. Inflammatory bowel disease was induced by the adoptive transfer of 6×10^5 naive CD4$^+$CD45RB^{hi} T cells (purified from C57BL/6 mice) into *Rag2*$^{-/-}$ mice by injection into the tail vein. Mice that received 1×10^5 expanded populations of CD4$^+$GFP$^+$ DEREG T_{reg} cells transduced with lentivirus containing control plasmid at the same time as the naive CD4$^+$CD45RB^{hi} T cells served as controls. For analysis of the function of SATB1-expressing T_{reg} cells, mice received 1×10^5 expanded populations of CD4$^+$GFP$^+$ DEREG T_{reg} cells transduced with lentivirus containing plasmid expressing SATB1 together with the naive CD4$^+$CD45RB^{hi} T cells. Recipient mice were weighed 3 times per week and monitored for signs of illness. After 9 weeks, mice were killed and the mesenteric and peripheral lymph nodes as well as spleens were analyzed by flow cytometry. For histological analysis, the large intestine (from the ileocecocolic junction to the anorectal junction) was removed, fixed in 10% (vol/vol) buffered formalin solution and processed for histological examination by routine procedures. Sections were stained with hematoxylin and eosin and assigned scores as described[54]. All samples were coded and assigned scores by researchers 'blinded' to the experimental conditions.

Assessment of histone modification in expanded human CD4$^+$ T cell populations. ChIP–quantitative PCR was done as follows. Expanded populations of T_{reg} and T_{conv} cells were collected, treated with micrococcal nuclease (to induce double-strand breaks in nucleosome linker regions), to generate approximately 80% mononucleosomes and 20% dinucleosomes. Chromatin from 2.5×10^6 cells was used for each ChIP experiment, which yielded approximately 500 pg DNA. Rabbit antibody to acetylated histone H4 (17-630), histone H3 trimethylated at Lys4 H3K4me3 (17-614) or histone H3 trimethylated at Lys27 (17-622; all from Millipore), as well as isotype-matched control antibodies, were used. SYBR green qPCR Master Mix (Fermentas) were used for PCR (primer sequences, **Supplementary Table 17**).

Statistical analysis. SPSS 19.0 software was used for Student's *t*-test and one-way analysis of variance with the least-significant-difference test.

Additional methods. Information on mice, reagents, antibodies, plasmids, experimental procedures and the generation of lentiviral vectors is available in the **Supplementary Methods**.

49. Brunkow, M.E. *et al.* Disruption of a new forkhead/winged-helix protein, scurfin, results in the fatal lymphoproliferative disorder of the scurfy mouse. *Nat. Genet.* **27**, 68–73 (2001).
50. Classen, S. *et al.* Human resting CD4$^+$ T cells are constitutively inhibited by TGF beta under steady-state conditions. *J. Immunol.* **178**, 6931–6940 (2007).
51. Sadlon, T.J. *et al.* Genome-wide identification of human FOXP3 target genes in natural regulatory T cells. *J. Immunol.* **185**, 1071–1081 (2010).
52. Wiznerowicz, M. & Trono, D. Conditional suppression of cellular genes: lentivirus vector-mediated drug-inducible RNA interference. *J. Virol.* **77**, 8957–8961 (2003).
53. Tang, Q. *et al.* In vitro-expanded antigen-specific regulatory T cells suppress autoimmune diabetes. *J. Exp. Med.* **199**, 1455–1465 (2004).
54. ten Hove, T. *et al.* Dichotomal role of inhibition of p38 MAPK with SB 203580 in experimental colitis. *Gut* **50**, 507–512 (2002).